Biomaterials Science

ROYAL SOCIETY OF CHEMISTRY

PAPER

View Article Online
View Journal | View Issue

Check for updates

Cite this: *Biomater. Sci.*, 2023, **11**, 3695

Optimization of 3D autologous chondrocyte-seeded polyglycolic acid scaffolds to mimic human ear cartilage†

Pedro Melgar-Lesmes, *[a,b,c] Oriol Bosch,[d] Rebecca Zubajlo,[a] Gemma Molins,[a] Sofia Comfort,[a] Ainara Luque-Saavedra,[d] Mario López-Moya,[a] Fernando García-Polite,[a] Francisco José Parri Ferrandis,[e] Carolyn Rogers,[f] Agata Gelabertó,[g] Jordi Martorell,[d] Elazer R. Edelman[a,h] and Mercedes Balcells[a]

Received 9th January 2023,
Accepted 13th March 2023

DOI: 10.1039/d3bm00035d

rsc.li/biomaterials-science

Auricular reconstruction in children with microtia is one of the more complex procedures in plastic surgery. Obtaining sufficient native material to build an ear requires harvesting large fragments of rib cartilage in children. Herein, we investigated how to optimize autologous chondrocyte isolation, expansion and re-implantation using polyglycolic acid (PGA) scaffolds for generating enough cartilage to recapitulate a whole ear starting from a small ear biopsy. Ear chondrocytes isolated from human microtia subjects grew slower than microtia rib or healthy ear chondrocytes and displayed a phenotypic shift due to the passage number. Rabbit ear chondrocytes co-cultured with mesenchymal stem cells (MSC) at a 50 : 50 ratio recapitulated the cartilage biological properties *in vitro*. However, PGA scaffolds with different proportions of rabbit chondrocytes and MSC did not grow substantially in two months when subcutaneously implanted in immunosuppressed mice. In contrast, rabbit chondrocyte-seeded PGA scaffolds implanted in immunocompetent rabbits formed a cartilage 10 times larger than the original PGA scaffold. This cartilage mimicked the biofunctional and mechanical properties of an ear cartilage. These results indicate that autologous chondrocyte-seeded PGA scaffolds fabricated following our optimized procedure have immense potential as a solution for obtaining enough cartilage for auricular reconstruction and opens new avenues to redefine autologous cartilage replacement.

Introduction

Pathologic ear development has profound physical and psychological effects. Microtia is a congenital malformation where the pinna (external ear) is underdeveloped and anotia involves a completely undeveloped pinna.[1] Microtia can be unilateral (one side only) or bilateral (both sides) and occurs in 1 out of about 8000–10 000 births.[2] The etiology of microtia in children remains unclear but it has been associated with genetic defects in different genes, gestational diabetes, or isotretinoin treatment during pregnancy.[1,3] Traditional reconstruction requires extraction of 4 costal cartilage segments (6th to 9th ribs) in children through a chest incision to obtain enough cartilage fragments for the surgeon to mold an ear backbone for a replica of a normal ear.[4,5] This construct is placed subcutaneously in the exact location of the future ear. Cartilage tissue is aneural and avascular. It is nourished by diffusion from the surrounding tissue vascular network.[6] Hence, both the cartilage used to reconstruct the ear and the cartilage in the chest incision survive and remain viable for an indefinite period. There is no other source of hyaline cartilage in the body with sufficient mass for an auricular reconstruction using autologous cartilage. Moreover, the regenerative capacity of the extracted fragments is limited by the dense extracellular matrix (ECM) and local restoration is never complete.[6]

Cartilage is a connective tissue composed of specialized cells called chondrocytes that produce a large amount of collagenous ECM.[7] Matrix properties are responsible for toughness and elasticity of cartilage tissue.[7] Cartilage ECM is

[a]*Institute for Medical Engineering and Science, Massachusetts Institute of Technology, Cambridge, MA, USA. E-mail: pedroml@mit.edu, pmelgar@ub.edu; Fax: +1 617-253-2514; Tel: +1 617-715-2026*
[b]*Department of Biomedicine, School of Medicine, University of Barcelona, Barcelona, Spain*
[c]*Biochemistry and Molecular Genetics Service, Hospital Clínic Universitari, IDIBAPS, CIBERehd, Barcelona, Spain*
[d]*Bioengineering Department, Institut Químic de Sarrià, Ramon Llull Univ, Barcelona, Spain*
[e]*Sant Joan de Deu Hospital, Barcelona, Spain*
[f]*Boston Children's Hospital, Boston, MA, USA*
[g]*Asociación Española de Microtia, Madrid, Spain*
[h]*Cardiovascular Division, Brigham and Women's Hospital and Harvard Medical School, Boston, MA, USA*
† Electronic supplementary information (ESI) available. See DOI: https://doi.org/10.1039/d3bm00035d

formed mainly by water, proteoglycans, elastin, and collagen.[8] Collagen type II is the main structural element of cartilage and is composed of three α1(II)-chains forming a homotrimeric triple helix morphologically and biomechanically similar to collagen I,[9] but with a higher content in residues that improve the interaction with proteoglycans.[10] Elastin fibers are aligned in a thin network of elastic fibers interspersed with collagen fibrils in the interterritorial zone contributing to tissue deformability in auricular cartilage.[11] Therefore, new-engineered cartilages for auricular reconstruction must comply with both requirements: enriched in collagen II fibers but sufficiently elastic for allowing deformation.

The use of cultured chondrocytes derived from autologous cartilage is an alternative to the need of processing atrial rib from the patient for auricular cartilage reconstruction. Different methodologies have been described for chondrocyte isolation from a tissue biopsy, growth, expansion, and construction of a new cartilage for implantation.[12,13] However, many investigations have used immunosuppressed mice as a model to implant chondrocyte-seeded scaffolds or hydrogels (*i.e.* PGA, polylactic acid, and combinations of both) and all of them do not achieve an adequate cartilage growth to accomplish the cartilage mass needed to reconstruct a full-size human ear. This is, in part, consequence of the reduced capacity of microtia chondrocytes for cartilage regeneration *in vivo* compared to healthy ear chondrocytes.[14] There is still a need for optimization and standardization of the passage number and adequate cell culture conditions to use autologous isolated human microtia chondrocytes for seeding tissue-engineered scaffolds for implantation.

Polyglycolic acid (PGA) scaffolds are absorbable, fibrous matrices with high surface area and superior void volume to promote natural tissue in-growth and cellular regeneration, and especially chondrocyte regeneration.[15] Currently, PGA materials are used in clinical applications for dental and pancreatic surgery,[16,17] as well as cardiovascular[18] and orthopedic tissue regeneration for arteries,[19] heart valves,[20] and cartilage.[21] The degradation product, glycolic acid, is nontoxic, and as it enters the tricarboxylic acid cycle can be excreted as water and carbon dioxide. A part of the glycolic acid is also excreted by urine.[22] In this investigation we chose this biocompatible biomaterial as scaffold for chondrocyte growth, subcutaneous implantation, and cartilage formation with the aim of optimizing the appropriate passage number and ideal conditions to maximize the growth of an auricular cartilage from a twice-folded PGA scaffold implant maintaining all the biofunctional properties.

Experimental

Chondrocyte isolation from ear or rib cartilage

In humans. Human auricular and rib cartilage were collected from 24 different children (age range, 7–12 years) at the Boston Children's Hospital and the Sant Joan de Déu of Barcelona Children's Hospital with informed consent. This protocol was approved by the Clinical Ethics Committee at the Hospital Sant Joan de Déu in Barcelona and Boston Children's Hospital. Samples obtained consisted of normal auricular cartilage, auricular cartilage with microtia, and rib cartilage from a total of 24 subjects. The perichondrium was removed under sterile conditions. A 0.5 × 0.3 cm wedge of human auricular cartilage was removed by a small retro auricular incision. This area is the easiest to access and with the lowest risk of keloid scarring. In this area there is cartilage even in the most complex forms of microtia and the scar created to remove it does not interfere with the subsequent reconstruction. The wound was subsequently sutured. Obtaining the biopsy did not lead to any functional or aesthetic sequels. The isolated cartilage was minced into small fragments and washed in PBS solution containing 100 units per mL of penicillin, 100 μg mL^{-1} of streptomycin and 0.25 μg mL^{-1} of Fungizone® Antimycotic following a standard chondrocyte isolation protocol.[23] Then, cartilage fragments were digested with 0.3% collagenase II for 5 h at 37 °C. The resulting cell suspension was filtered with a sterile 100 μm cell strainer and centrifuged at 225 Gs for 5 min. The cell pellet was suspended in Ham's F-12 medium and plated into a 25 cm^2 cell culture flask at a density of 20 000 to 30 000 cells per cm^2.

In rabbits. Four New Zealand white rabbits were used to obtain four biopsies per animal with a 6 mm biopsy punch. The biopsies were obtained from each side of the ear artery. Chondrocytes were isolated by collagenase digestion as described above and used for *in vitro* assays, for implantation of chondrocyte-seeded PGA scaffolds in immunodeficient mice or for implantation in the same immunocompetent rabbits (autologous implants).

Cell culture

Human or rabbit chondrocytes were seeded in 25 cm^2 cultured flasks in a humidified Thermo Scientific Forma Series II Water Jacket CO_2 incubator in chondrocyte culture medium: Ham's F12 culture medium with L-glutamine, 25 μg mL^{-1} of L-ascorbic acid, 100 units per mL of penicillin, 100 μg mL^{-1} of streptomycin, 0.25 μg mL^{-1} of Fungizone® Antimycotic (AM) and 10% FBS. The culture medium was changed twice a week. To optimize the culture, an MTS assay was performed with different chondrocyte medium compositions: Ham's F12, 1% AM (Invitrogen, Life Technologies, Carlsbad, CA, USA), 25 μg mL^{-1} ascorbic acid (Sigma-Aldrich, USA), different concentrations of fetal bovine serum (FBS, Lonza, Walkersville, MD, USA) and the presence or absence of basic fibroblast growth factor (b-FGF at 10 ng mL^{-1}, R&D Systems Inc, Minneapolis, Minn, USA) to find the best option for chondrocytes culture (10% FBS + b-FGF). MSC were cultured with DMEM media supplemented with 100 units per mL of penicillin, 100 μg mL^{-1} of streptomycin, 0.25 μg mL^{-1} of AM and 10% FBS.

Chondrocyte seeding in PGA scaffolds

The PGA three-dimensional scaffold (fiber diameter: ≈15 μm) is only made of poly[oxy(1-oxo-1,2-ethanediyl)] purchased from Biomedical Structures LLC and sourced from Teleflex Medical (Biofelt™). The PGA scaffold is a non-woven, absorbable, com-

mercial fibrous matrices with high surface area and superior void volume to promote natural tissue in-growth and cellular regeneration at the site of surgery or damage. The PGA scaffold is stored in a desiccator until usage to prevent hydrolysis. For human or rabbit-derived cell seeding, the scaffold is cut in 2 × 2 cm squares, which are placed in cell culture well plates and treated overnight with 70% ethanol for sterilization. Following 5 washes with sterile PBS, either chondrocytes or MSC (50 million cells per cm^3 scaffold) were seeded in the above-described 3D PGA scaffold at different concentrations and proportions and, after adhering for 48 h in a humidified Thermo Scientific Forma Series II Water Jacket CO_2 incubator, they were subcutaneously implanted in animals. Experiments seeding PGA scaffolds with human or rabbit chondrocytes or MSC were performed in quadruplicates.

Western blot

Non-specific cell lysis was performed in isolated human chondrocytes (passage 1, 2, and 5) by rinsing cells twice with ice cold PBS and then incubating them for 30 min on ice in RIPA buffer containing 50 mM Tris-HCl, pH 7.4, 150 mM NaCl, 1% NP-40, 0.5% sodium deoxycholate, 0.1% SDS and 5 mM EDTA. The supernatant was extracted after centrifugation for 30 min at 13 000*g* and 4 °C, and mixed with 1 : 4 v/v of Laemmlli's buffer (Boston Bioproducts, Boston, MA) with 8% mercaptoethanol (Sigma). 10% acrylamide gels (Life Technologies) were used for protein separation. Gels were blotted using Life Technologies gel transfer stacks and blotting system. Membranes were blocked with 5% powdered milk and incubated overnight at 4 °C while shaking with the antibodies of interest at a 1 : 1000 dilution (Collagen I, II and Elastin, Abcam, Cambridge, USA). After two washes with PBS-T (PBS, 0.05% Tween 20, Sigma), membranes were incubated with appropriate HRP-conjugated secondary antibodies diluted 1 : 2000 for 1 h while shaking at room temperature. After two 10 min washes in PBS-T, LuminataTM Forte Western HRP Substrate (Milipore, Billerica, MA) was applied and luminescence was detected in a Chemidoc XRS + (Bio-Rad, Hercules, CA).

Immunofluorescence, elastin, and proteoglycans staining

Cellular functionality was assessed using immunofluorescence (IF), elastin and Safranin O (for proteoglycans) staining in cells in culture for 3 or 4 weeks. For IF, cell constructs were rinsed with PBS and fixed with 4% paraformaldehyde (PFA, Sigma) for 30 minutes at room temperature. Excessive aldehydes were quenched with 0.2M glycine in PBS for 10 minutes and, after washing with PBS, cells were permeabilized with 0.2% X-100 Triton in PBS for 10 minutes. After two consecutive washes with PBS for 10 minutes and 1 hour blotting with 5% goat serum in PBS-BSA (PBS, 1% bovine serum albumin, Sigma), cells were labeled overnight at 4 °C with their respective antibodies (collagen I, collagen II, heparan sulfate, and chondroitin sulfate from Abcam, Cambridge, MA, USA), diluted 1 : 50 in PBS-BSA. Cells were rinsed twice with PBS-BSA for 10 minutes and stained with the appropriate secondary antibodies and DAPI solution (1 : 100 in PBS-BSA) for 2 h. Two additional 10 minutes washes with PBS were performed to remove any unbound antibody. Specimens were imaged using a Nikon (Tokyo, Japan) Eclipse TI-E epifluorescence microscope or a PerkinElmer (Waltham, MA) spinning disk confocal system coupled to a Zeiss (Jena, Germany) Axiovert 200M microscope. For elastin immunocytochemistry, cells were rinsed with PBS and fixed with 4% paraformaldehyde (PFA, Sigma) for 30 minutes at room temperature. Excessive aldehydes were quenched with 0.2M glycine in PBS for 10 minutes. Afterwards, cells were permeabilized with 0.2% X-100 Triton in PBS for 10 minutes, washed twice with PBS and endogenous peroxidase activity was inhibited for 10 minutes with 3% hydrogen peroxide. After two consecutive washes with PBS for 10 minutes and 1 hour blotting with 5% goat serum in PBS-BSA (PBS, 1% bovine serum albumin, Sigma), cells were labeled overnight at 4 °C with rabbit polyclonal antibodies anti-elastin 1 : 200 (Abcam, Cambridge, MA, USA). The samples were revealed with the Dako LSAB2 and HRP/DAB System (Dako Denmark A/S, Glostrup, Denmark) following the manufacturers' instruction. Controls were performed by omitting the first antibody. Immunoreactivity was visualized by light microscope (Olympus Bx51, Tokyo, Japan). For Safranin O staining, cell samples were first stained with Weigert's iron hematoxylin solution for 10 minutes and washed in running tap water for 10 minutes. Then, samples were stained with 0.05% fast green solution for 5 minutes and rinsed quickly with 1% acetic acid solution for 10 seconds. Samples were then stained in 0.1% safranin O solution for 5 minutes and dehydrated with 95% ethyl alcohol, absolute ethyl alcohol, and xylene, using 2 changes each, 2 minutes each. Cell preparations were then mounted using resinous medium Pertex and visualized by light microscope (Olympus Bx51, Tokyo, Japan).

Perfusion system for cell-seeded scaffolds

A customized perfusion system was built as previously described.[24] Briefly, chondrocyte-seeded PGA scaffolds were sutured to 7 cm diameter tubes into a plastic reservoir and connected to a 60 cm-long loop of silastic tubing (Dow Corning, Medford, MA) containing fresh Ham's F12 medium. These tubes were connected to a perfusion pump and exposed to a continuous shear stress corresponding to 50 rpm (2 dyne per cm^2). Every 2 weeks 100 mL of media was replaced by fresh media. After 8 weeks, scaffolds were imaged under bright field microscopy and fixed with PFA 4%. Three small pieces (1 cm^2) of the resulting grown mass were used for the staining with anti-collagen I and anti-collagen II (1 : 50, ThermoFisher Scientific, USA) and anti-Heparan Sulfate (1 : 50, Millipore, UAS). Samples stained positive for collagen I, collagen 2 and heparan sulphate. PGA controls without cells degraded completely.

Characterization of chondrocyte-seeded PGA scaffolds under flow

Chondrocyte-seeded PGA scaffolds were imaged under bright field microscopy and fixed with PFA 4%. Three small pieces (1 cm^2) of the resulting mass were used for the immunofluorescent staining with anti-collagen I, anti-collagen II (1 : 50,

Abcam, Cambridge, USA), and anti-Heparan Sulfate (1 : 50, Millipore, USA) using a multiphoton microscope (Leica Microsystems, Heerbrugg, Switzerland). The whole collagen matrix structure was obtained by the second harmonic in multiphoton fluorescent microscopy.

Subcutaneous implantation and extraction of chondrocyte-seeded PGA scaffolds

All the animal experiments were approved by the Animal Ethics Committee at Massachusetts Institute of Technology, MA, USA.

Immunodeficient mice. PGA scaffolds (0.5 × 0.5 × 0.2 cm) were seeded at a concentration of 50 million cell per cm^3 using rabbit chondrocytes or MSC. Rabbit chondrocytes were isolated as described above. Bone marrow MSC were isolated as previously described.[25] Briefly, bone marrow was obtained as a source of MSC by puncturing a rabbit iliac crest with a 16G needle and 1.5 ml syringe previously coated with 0.5 mL heparin to prevent coagulation. Then, 1 mL of bone marrow was diluted in 9 mL of DMEM media supplemented with 10% FBS and plated in a cell culture flask for 5 days. Media was replaced, and the remaining adherent cells were of mesenchymal origin expressing cell surface markers such as CD44, CD105 and CD90 (data not shown). Some of the scaffolds were seeded with 100% rabbit chondrocytes and some with 100% rabbit MSC (n = 4 in every group). Other scaffolds were seeded with different ratios Chondrocyte : MSC (75 : 25, 50 : 50, 25 : 75; n = 4 per condition) following previous *in vitro* studies that explored these two different cell types as sources of tissue engineered cartilage. Implants were kept in the incubator for a total of 3 days under static conditions and then implanted subcutaneously in the dorsum of male SCID hairless congenic mice (SHC Mouse CB17. Cg-PrkdcscidHrhr/IcrCrl from Charles River Laboratories International, 6 weeks) for 2 months (4 animals per condition, plus one control animal with implant without cells).

Immunocompetent rabbits. PGA scaffold was cut in square-shape 1 cm^3 samples (2cm × 2cm × 0.25 cm, length × width × height, L × W × H) and treated with 1 mL 70% ethanol overniRabbit chondrocytes were seeded and grown as described above, and squares were folded twice to form a compact 3D square-shape mass to be subcutaneously implanted. The implantation site was shaved and cleaned with several cycles of betadine scrub followed by 70° alcohol rinse. Two 1.5 cm incision were performed in the animal's dorsum to create a subcutaneous cavity. The preformed PGA construct was placed in this space, after which each skin incision was closed with 4.0 nylon sutures as in the following scheme of a rabbit back:

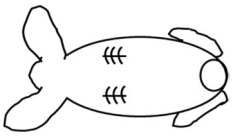

Two PGA constructs were implanted per animal to reduce the number of animals (4 animals were used in this experiment). Glycopyrrolate (0.1 mg kg^{-1} IM) was used as a pre-anesthetic and Buprenex/Meloxycam 0.05 mg kg^{-1} subcutaneously as pain killers for the surgery. Anesthesia was induced by ketamine 35–50 mg kg^{-1} and xylazine 5–10 mg kg^{-1} IM with a maintenance with ~2% isoflurane from a calibrated vaporizer with endotracheal intubation. Implantation sites were assessed rigorously (at least daily) for the first week following implantation of the scaffold for signs of edema, erythema, or infection and animals were monitored for signs of distress or pain. Sutures were removed after 14 days. Animals were euthanized at 1 and 2 months following the implantation surgery to remove the subcutaneous cartilaginous materials formed.

Biological characterization of rabbit explants

For analysis of cartilage phenotype in rabbit explants, they were fixed in 4% formaldehyde overnight at room temperature. Then, explants were embedded in paraffin to perform 5 μm tissue sections for histology. Sections of the explants were deparaffinized following a xylene-ethanol protocol and underwent antigen retrieval with 1% SDS solution for 5 min at room temperature. Then they were blocked with 5% normal goat serum, and incubated with anti-collagen I, anti-collagen II (1 : 50, Abcam, Cambridge, USA). In addition, 4′,6-diamidino-2-phenylindole (DAPI, Vectashield, Vector laboratories, Burlingame, CA) was used to counterstain cell nuclei. Controls without primary antibodies were used as negative controls. Binding sites of the primary antibodies were revealed with Cy3-conjugated goat-anti-mouse IgG (Jackson ImmunoResearch Laboratories, West Grove, PA, USA) incubated for 1 h at room temperature. Samples were visualized with an epifluorescence microscope (Nikon Eclipse Ti, Kanagawa, Japan). Volume of implants and explants of chondrocyte-seeded PGA scaffolds was calculated as L × W × H.

Mechanical tests

Tension/elongation tests were performed in rabbit ear cartilage, unseeded PGA scaffolds and explants after 1 or 2 months from implantation using compressive and tensile modes of a universal testing machine (Instron 5984; Instron, Norwood, MA, USA) and Software (Bluehill® version 2.0; Instron) to record the force value with a 1 kN load cell and 150 kN capacity.

Statistical analysis

Data were analyzed using GraphPad Prism® 8.0 and expressed as mean ± standard error. Statistical analysis of the results was performed by one-way ANOVA and the Tukey *post-hoc* test, and the unpaired Student's t test when appropriate. Differences were considered significant at a p value of 0.05 or less.

Results

Optimization of isolated human ear chondrocyte expansion with phenotype preservation

Harvesting of microtia cartilage required precise surgery as the microtia cartilage was extremely irregular-shaped and the sur-

rounding fibrous tissue was very dense. Indeed, the complete removal of fibrous tissue including perichondrium was critical to guarantee high purity of microtia chondrocytes (MCs) for latter experiments. In our protocol, around 2 million MCs could be initially isolated from a ≈6 mm biopsy from microtia cartilage. Isolated MCs (passage 0) presented as round or polygon morphologies similar to normal auricular chondrocytes under light microscope (Fig. 1A and B). No visual changes in ear MCs size and morphology were observed during the first passage (Fig. 1A).

However, most ear MCs switched their morphology after passage 2 displaying a flat and elongated fibroblastic-like cell shape, something not found in healthy chondrocytes until passage 4 (Fig. 1A and B). Rib MCs preserved size and morphology from passage 0 to 4 in a similar fashion to healthy chondrocytes (Fig. 1C). Moreover, proliferation of rib MCs was faster than ear MCs or healthy chondrocytes after 1 day of cell culture (Fig. 1D). After 2 days of cell culture, healthy and rib MCs proliferated proportionally, and ear MCs were always slower until day 5 when all three chondrocyte proliferations leveled (Fig. 1D). To find out the best combination of growth factors to optimize the ear MCs growth, we quantified ear MCs proliferation in cell cultures with different percentages of FBS (0, 5 and 10%) in the presence or absence of b-FGF for 5 days. We found that proliferation increased when FBS percentage was higher (from day 1 to 5) and the addition of the chondrocyte mitogenic factor b-FGF allowed reaching the proliferation peak two days faster than chondrocytes incubated without it (Fig. S1†). Therefore, the combination of 10% FBS + bFGF (10 ng mL^{-1}) optimized *in vitro* human ear MCs proliferation. The biological properties of isolated ear MCs were also analyzed to assess the passage number limiting the biofunctional phenotype preservation. We found that elastin expression (a crucial protein for cartilage elasticity) drastically decreased after passage 1 and disappeared in passage 5, while healthy chondrocytes and even rib MCs preserved some elastin expression after passage 2 (Fig. 2A).

We also analyzed collagen I expression in isolated human ear MCs as it is known that the synthesis of collagen I is an indicator of chondrocyte transdifferentiation into fibroblastic-like cells.[26] We observed low collagen I expression at passage 2 that considerably increased at passage 5 in ear MCs, and this

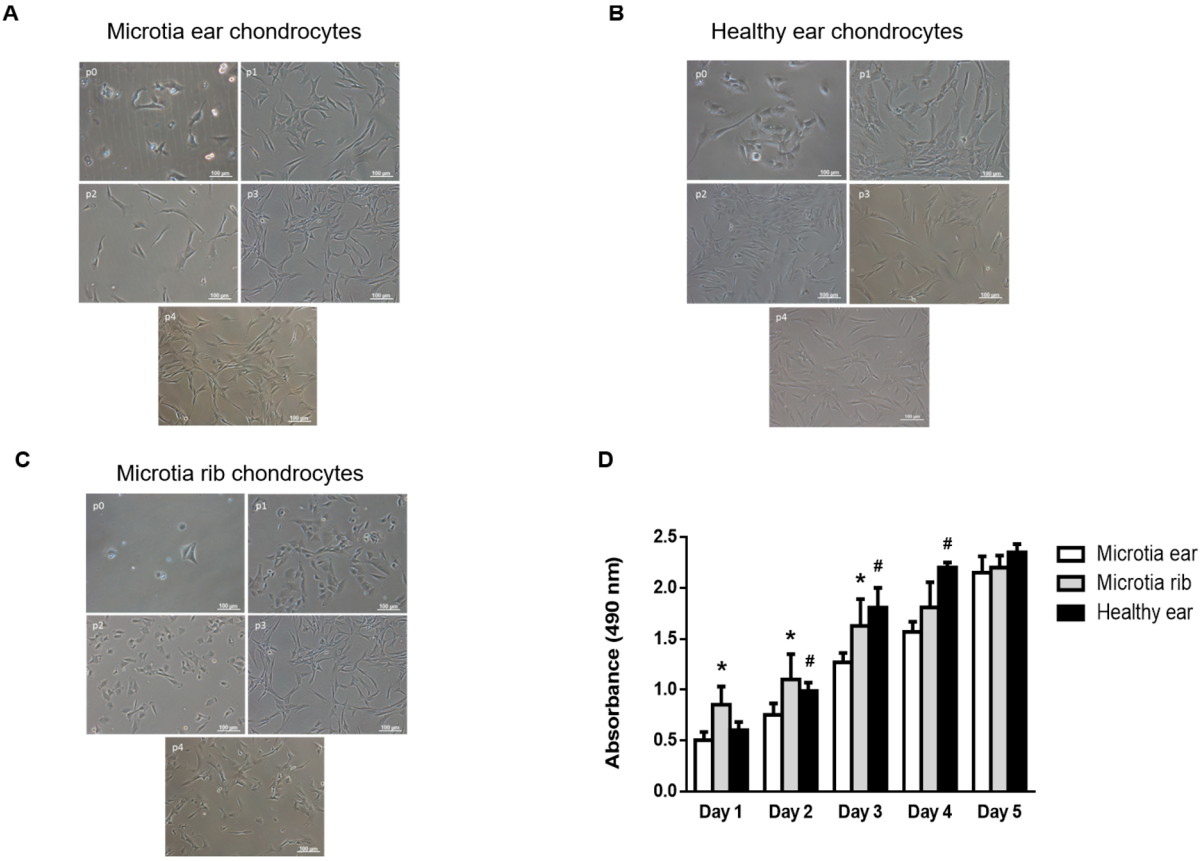

Fig. 1 Comparative behaviour in growth and morphology between isolated healthy or diseased chondrocytes over time and according to the passage number. (A) Bright field images showing the cell morphology at different passages of human chondrocytes isolated from the ear of a patient with microtia. (B) Bright field images showing the cell morphology at different passages of human healthy chondrocytes isolated from the ear. (C) Bright field images showing the cell morphology at different passages of human chondrocytes isolated from the rib of a patient with microtia. (D) Results of the cell growth kinetics using MTS assay obtained from isolated healthy, microtia ear, or microtia rib chondrocytes specific medium supplemented with 10% FBS for 5 days. Histograms are plotted as mean ± SEM. *$p < 0.05$ *vs.* microtia ear; #$p < 0.05$ *vs.* microtia ear.

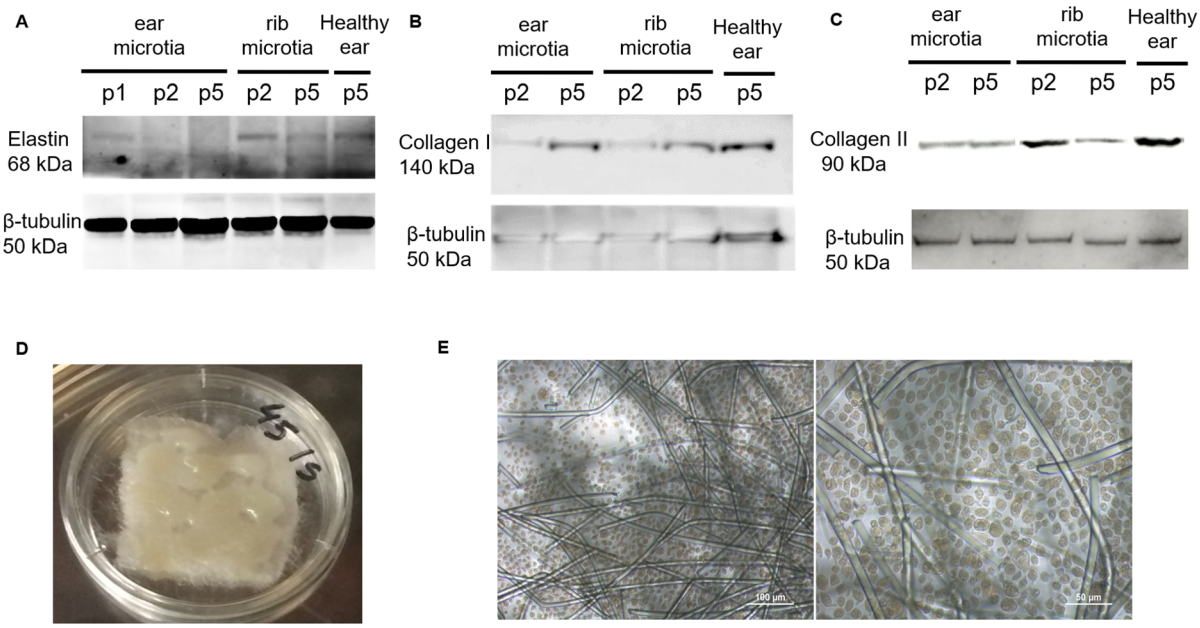

Fig. 2 Effects of passage number on biofunctional behaviour of isolated healthy or diseased chondrocytes to optimize scaffold seeding. (A) Elastin expression was analysed *via* western blot in isolated healthy, microtia ear, or microtia rib chondrocytes after different passage numbers. (B) Collagen I expression was analysed *via* western blot in isolated healthy, microtia ear, or microtia rib chondrocytes after different passage numbers. (C) Collagen II expression was analysed *via* western blot in isolated healthy, microtia ear, or microtia rib chondrocytes after different passage numbers. (D) Macroscopic aspect of a PGA scaffold seeded with human ear microtia chondrocytes growing at passage 2. (e) Morphology of human ear chondrocytes from passage 2 growing in a PGA scaffold for 1 month analysed *via* light microscopy (20× magnification).

also occurred in healthy and rib MCs (Fig. 2B). In contrast, collagen II, the main structural element of cartilage, was abundant in healthy ear and rib MCs at low passage (p2) but scant in the rib MCs at higher passages (p5) (Fig. 2C). Although ear MCs showed less collagen II expression at passage 2, this was preserved at passage 5 (Fig. 2C). According to these outcomes, passage 2 and the selected chondrocyte culture medium were considered the optimal conditions to seed PGA scaffolds. Indeed, ear MCs grew uniformly in the material (Fig. 2D), displaying a typical round or polygon morphology analogous to normal chondrocytes in an auricular cartilage (Fig. 2E).

Validation of the chondrocyte expansion method in rabbits prior to implantation

To verify chondrocyte-seeded PGA scaffold implantation methods in patients with microtia, we used isolated ear rabbit chondrocytes (RCs) following the same procedures as described for human MCs. Isolated chondrocytes from a 6 mm biopsy from the rabbit ear demonstrated no presence of collagen I and a high content of collagen II with a dense network of heparan sulfate (key player in cartilage biology) (Fig. 3A).

After two passages, collagen I appeared slightly expressed whereas collagen II and heparan sulfate maintained the levels of protein expression (Fig. 3B). Collagen I expression rose with every passage until passage 5, while collagen II and heparan sulfate were barely present at that passage and collagen I was predominant, denoting a chondrocyte transdifferentiation to fibroblastic-like cell types (Fig. 3C and D). These outcomes validated that passage 2 was a good threshold to be selected as optimal passage number for seeding chondrocytes on PGA scaffolds, as we confirmed in chondrocyte-seeded PGA scaffolds (Fig. 3E). We additionally investigated whether continuous shear stress that occurs to chondrocyte-seeded scaffolds over time in the subcutaneous implantation could have an impact on the expression of biofunctional markers of cartilage chondrocytes. For this reason, we designed a customized bioreactor perfusion system to expose rabbit chondrocyte-seeded PGA scaffolds to cell culture medium flow (Fig. S2A†). As occurred with MCs PGA scaffolds, rabbit chondrocyte-seeded PGA scaffolds displayed the typical round or polygon morphology (Fig. S2B†). Interestingly, after 8 weeks of incubation under a cell culture medium flow of 4 mL min^{-1}, rabbit chondrocytes in PGA scaffolds displayed a dual phenotype: on one side corresponding to cartilage chondrocytes because of the high presence of collagen II and heparan sulfate; and, on the other side, with some feature of fibroblastic-like cell types due to the high presence of collagen I (Fig. S2C†).

Evaluation of the biofunctional properties of isolated rabbit chondrocytes in co-culture with MSC (MSC)

Our experiments using rabbit chondrocytes under shear stress made us hypothesize that chondrocytes in cartilage might also need the assistance of surrounding MSC (that synthesize collagen I) to give mechanical support. Indeed, some publications have described implantable systems using a combination of

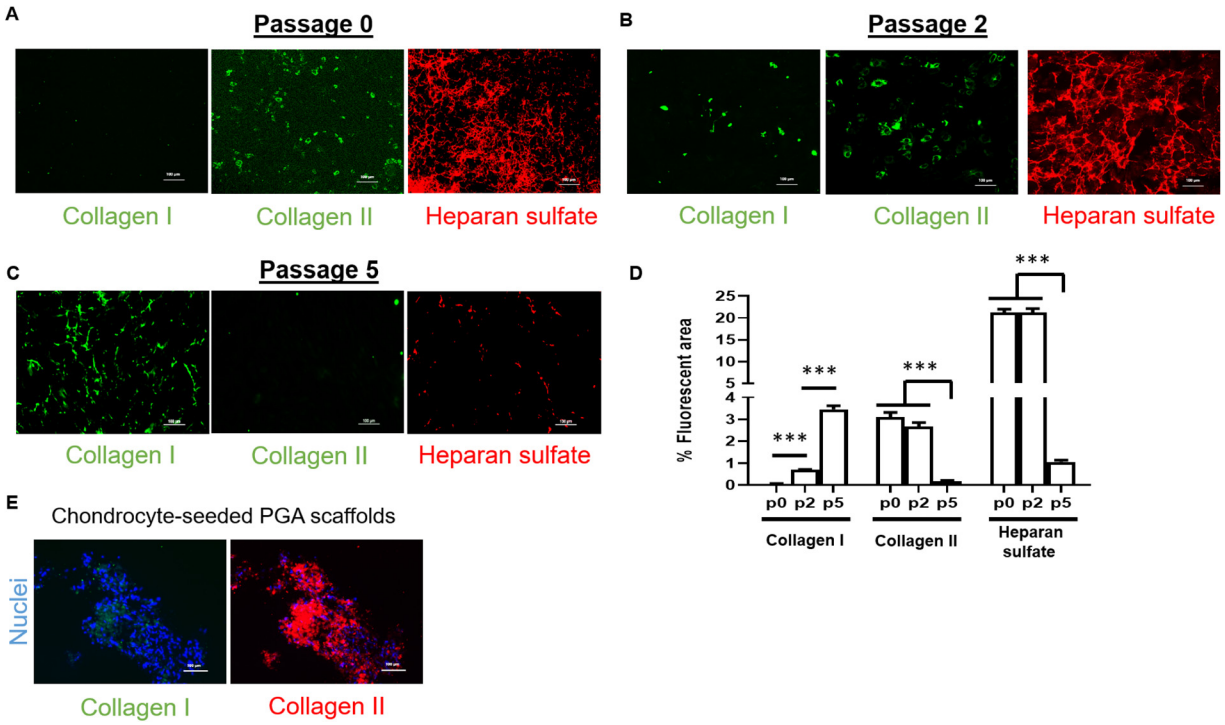

Fig. 3 Effects of passage number on cartilage markers in isolated rabbit chondrocytes. Study of passage number effects on biofunctional behaviour of isolated healthy or diseased chondrocytes to optimize scaffold seeding before animal experiments. (A) Collagen I, II and heparan sulfate (Col I, Col II and HS, respectively) expression and localization in isolated rabbit chondrocytes. (B) Collagen I, II and heparan sulfate expression and localization in rabbit chondrocytes after 2 passages. (C) Collagen I, II and heparan sulfate expression and localization in rabbit chondrocytes after 5 passages. (D) Quantification of percentage of fluorescent area from immunofluorescence images obtained for collagen I, II, and heparan sulfate (n = 4 per passage); data are represented as mean ± SEM. Significant differences between the groups: ***p < 0.001. (E) Collagen I and II expression in PGA scaffolds seeded with rabbit chondrocytes at passage 2. All images were obtained *via* epifluorescence microscopy (20× magnification).

mesenchymal cells and chondrocytes for cartilage regeneration.[25,27,28] For this reason, we evaluated the impact on chondrocyte biofunctional properties of co-culturing isolated rabbit chondrocytes with different proportions of MSC. An equal balance of chondrocytes and MSC (50 : 50) was optimal, maintaining the elastin expression in chondrocytes for three or four weeks (Fig. 4A).

Similarly, collagen II expression was maintained in co-cultures of chondrocytes and MSC at 50 : 50 ratio for three weeks and this drastically dropped when the MSC proportion increased (Fig. 4B). As glycosaminoglycans (GAG) and proteoglycans represent the second largest group of macromolecules in cartilage that confer resistance to compressional forces in cartilage,[29] we also evaluated their abundance in co-cultures of chondrocytes and MSC. Although proteoglycans stained by Safranin O did not appear in abundance in the 50 : 50 chondrocyte/MSC ratio after three weeks of co-culture, we found a strong up-regulation and proteoglycan synthesis in the chondrocyte/MSC co-culture at this ratio after four weeks of incubation (Fig. 5A).

As expected, total cartilaginous GAG content quantified by the Blyscan assay resulted more abundant in all cell cultures containing chondrocytes, but only the 50 : 50 chondrocyte/MSC ratio showed no significant differences with the GAG synthesis in cell cultures with only chondrocytes (Fig. 5B). One of the most characteristic GAG in chondrocytes is chondroitin sulfate. Our results indicate that chondroitin sulfate abundance is maintained in the 50 : 50 chondrocyte/MSC ratio after three weeks of co-culture and decreases afterwards (Fig. 5C). Therefore, we hypothesized that rabbit chondrocytes and MSC seeded at a 50 : 50 ratio in PGA scaffolds should be the optimal proportion for subcutaneous implantation to obtain a rapid *in vivo* growth of new cartilage mass that recapitulates all the biological properties of the original cartilage.

Rabbit chondrocyte-seeded PGA scaffolds implanted in immunodeficient mice did not grow faster in co-culture with MSC

We subcutaneously implanted PGA scaffolds seeded with different rabbit chondrocyte/MSC ratios in immunodeficient mice to investigate whether we can use the subcutaneous tissue as a bioreactor to obtain enough cartilaginous mass for auricular reconstruction. We used mice as a small animal model for a first trial. As cells were from a different species, we had to use immunodeficient mice to avoid implant rejection. The PGA implant represented approximately a third of the mouse dorsal surface (Fig. 6A).

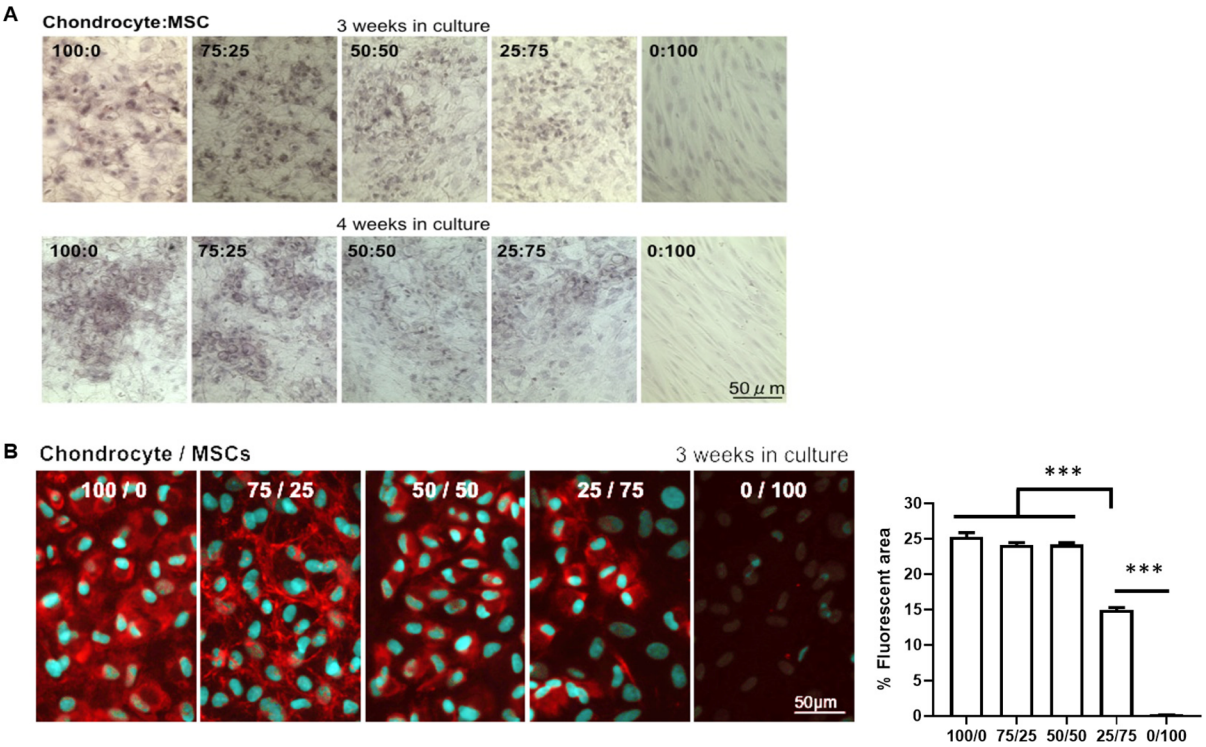

Fig. 4 Biofunctional properties of isolated rabbit chondrocytes in co-culture with MSC. (A) Elastin staining in isolated ear rabbit chondrocytes in co-culture with MSC at different ratios (B) Collagen II fluorescent staining in isolated ear rabbit chondrocytes in co-culture with MSC at different ratios. Quantification of percentage of fluorescent area is represented as mean ± SEM. Significant differences between the groups: ***$p < 0.001$.

Implants with all the combinations of rabbit chondrocyte/MSC ratios were extracted two months after implantation and measured with a micrometer ruler (Fig. 6B). Although we observed a trend to size increase in explants containing chondrocytes, no significant growth was found between PGA scaffolds without cells or with any rabbit chondrocyte/MSC ratio (Fig. 6C). Therefore, the addition of MSC to rabbit chondrocyte-seeded PGA scaffolds did not improve cartilage growth *in vivo* indicating that the immune system might be needed for regeneration after implantation of cell-seeded scaffolds as some publications have recently pointed out.[30–32]

Implants of chondrocyte-seeded PGA scaffolds allowed obtaining enough cartilaginous mass to recapitulate a whole ear in immunocompetent rabbits

The absence of cartilage growth in immunodeficient mice indicated that the implantation of rabbit chondrocyte-seeded PGA scaffolds in immunocompetent rabbits could overcome the limitations of lacking the influence of the immune system to stimulate cartilage growth and with a higher surface area than in mice. We selected 100% chondrocyte-seeded PGA scaffolds because the combination with MSC did not show a high cartilage growth in implanted mice. We hypothesized that subcutaneous tissue may provide an optimal cell niche, including the presence of host MSC, to create an ideal environment to boost chondrocyte growth and cartilaginous tissue formation with a specific ECM conformation for mechanical support.[25,27,28] We designed a very specific protocol considering all the information that we obtained isolating and expanding MCs and the implantation of rabbit chondrocytes in mice. We first obtained a small ear sample (6 mm) from rabbits with a biopsy punch (Fig. 7A).

Then we cleaned, washed, and isolated the ear cartilage (Fig. 7B). Cartilage was digested with collagenase to obtain rabbit chondrocytes for *in vitro* growth and expansion as described for MCs (Fig. 7C). Then, chondrocytes were seeded and grown on PGA scaffolds until full surface coverage and then, we folded twice the chondrocyte-seeded PGA scaffold to create a multilayer 3D chondrocyte environment (Fig. 7D) to be implanted subcutaneously in the dorsum of rabbits (Fig. 7E). After 1 or 2 months. newly formed cartilaginous tissue was extracted and surgically cleaned (Fig. 7F). The cleaned and isolated cartilaginous tissue formed at 1 or 2 months after implantation was used to test the biofunctional and mechanical properties in relation to a rabbit ear cartilage (Fig. 7G). The volume of the obtained cartilaginous explants was seven-fold higher after 1 month and almost ten-fold higher after two months than chondrocyte-seeded implanted scaffolds (Fig. 8A).

Therefore, the biggest explants in terms of mass and volume were found after two months of implantation. We then analyzed the collagen composition and structure of these explants in comparison to the cartilage from a rabbit ear. We observed a dense network of collagen II in both 1- and

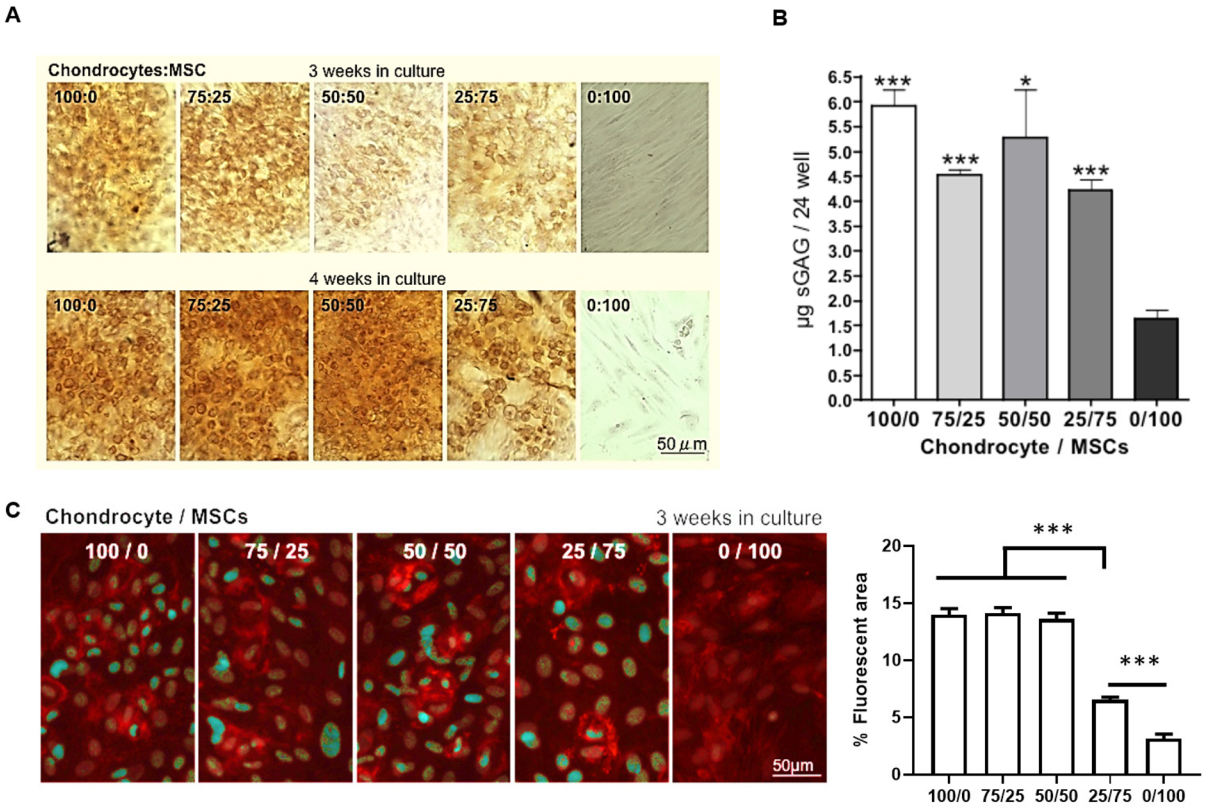

Fig. 5 Effects on cartilage proteoglycan content of co-culturing isolated rabbit chondrocytes with MSC. (A) Safranin O staining for the total cartilaginous proteoglycans content in isolated ear rabbit chondrocytes in co-culture with MSC at different ratios. (B) Quantification of total cartilaginous glycosaminoglycan content by the Blyscan assay in isolated ear rabbit chondrocytes in co-culture with MSC at different ratios. Data are plotted as mean ± SEM. Significant differences between the groups and 0/100 ratio: *$p < 0.05$; ***$p < 0.001$. (C) Chondroitin sulfate fluorescent staining in isolated ear rabbit chondrocytes in co-culture with MSC at different ratios. Quantification of percentage of fluorescent area is represented as mean ± SEM. Significant differences between the groups: ***$p < 0.001$.

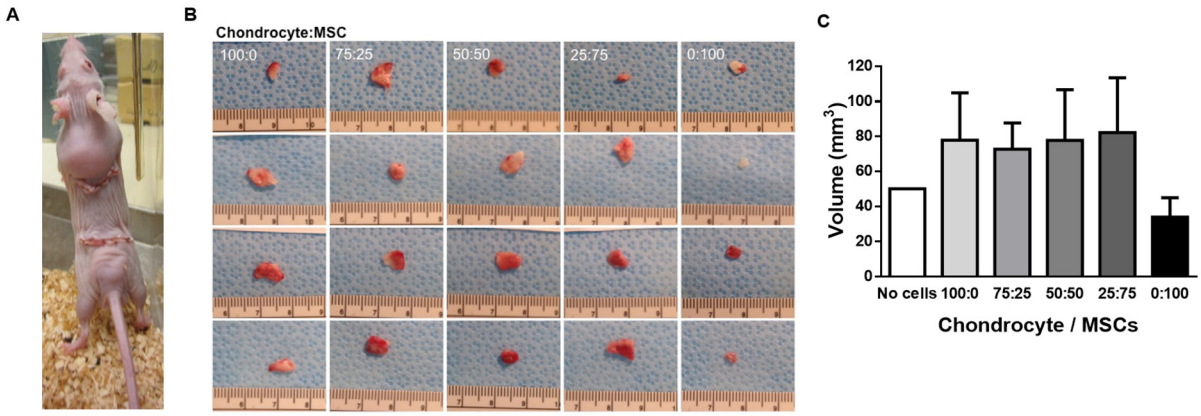

Fig. 6 Effects of subcutaneously implanting PGA scaffolds seeded with co-cultures of isolated rabbit chondrocytes and MSC in nude mice. (A) Anatomical localization and visual size of cell-seeded PGA scaffolds 2 months after implantation (B) Macroscopic aspect and visual size of explants obtained after 2 months of implantation of isolated ear rabbit chondrocytes seeded in PGA scaffolds in co-culture with MSC at different ratios. Ruler is shown below in cm. (C) Quantification of explant sizes obtained after 2 months of implantation of isolated ear rabbit chondrocytes seeded in PGA scaffolds in co-culture with MSC at different ratios. Data are plotted as mean ± SEM.

2-month explants that structurally mimicked the typical round or polygon morphology of an ear cartilage (Fig. 8B). Low levels of collagen I were found in both 1- and 2-month explants as occurred in ear cartilage (Fig. 8B). However, collagen II fibers in both explants were not as dense as in ear cartilage, although a higher density and complexity was found in the 2-month

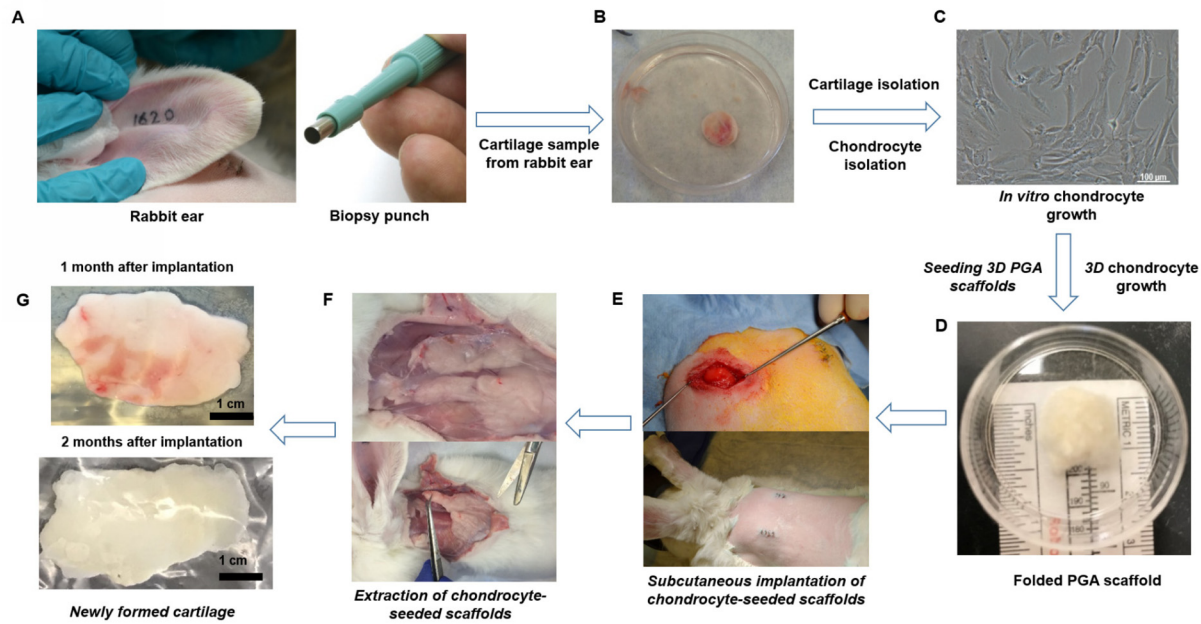

Fig. 7 Proceeding to obtain high mass of autologous cartilage using PGA scaffolds seeded with isolated ear chondrocytes. (A) A 6 mm biopsy was obtained from the rabbit ear using a biopsy punch (B) A 6 mm circular sample was obtained from the rabbit ear and washed, and the skin was removed to obtain isolated cartilage. (C) Completely clean ear cartilage was digested to isolate chondrocytes. A representative picture of isolated chondrocytes growing is shown. (D) Chondrocytes (5×10^7 cells) at passage 1 were seeded in 1 cm^3 PGA scaffolds, grown in cell culture plates for 48 h and then folded two times to form a tridimensional square. (E) Two 3D chondrocyte-seeded PGA scaffolds were then subcutaneously implanted in both dorsal sides of immunocompetent rabbits. (F) After 1 or 2 months, animals were euthanized and both grown tissues were clearly visualized under the skin and extracted to purify the cartilage. (G) Cartilaginous tissues formed from the subcutaneously implanted chondrocyte-seeded PGA scaffolds were isolated and cleaned for further analysis.

explants (Fig. 8B). Indeed, the alignment of collagen fibers in both 1-month and 2-month explants was very similar to the fibers in a rabbit ear cartilage although collagen bundles appeared much thicker and complex in the rabbit ear cartilage (Fig. S3†). The mechanical tensile test showed that both explants (at one or two months) displayed similar mechanical strength but very different to the initial PGA scaffold and lower but close to the mechanical properties of an ear cartilage (Fig. 8C).

Discussion

Microtia is a low-incidence congenital deformity that is usually not discovered on a prenatal ultrasound.[2] Fortunately, medical technology is advancing, and an ear can be successfully imitated using a prosthesis or rib cartilage and reconstruction. However, the amount of required harvested rib cartilage is high, pushing back the age of reconstruction until 10 years of age or older.[33] Ribs are the only source of hyaline cartilage in the body with enough mass for an autologous auricular reconstruction, but invasive surgery with different stages has meant an arduous physical and psychological endeavor for both children and their parents. Harvest of enough cartilage to build an ear requires a long incision on the chest leaving a long and sometimes unaesthetic scar. This is a fairly painful procedure and children can have tenderness in this area for up to a year or two post-surgery. Harvesting rib cartilage implies a risk of pneumothorax or leakage of air from the lungs, which can require placement of a chest tube or other invasive procedures. Furthermore, cartilage is "borrowed" to build an ear at the expense of leaving behind donor site deformity due to lack of cartilage in the chest. Herein, we describe how to optimize the isolation and expansion of ear MCs from a small size ear sample to avoid the harmful effect of harvesting from rib cartilage. Some authors have described the use of even passage 5 MCs for ear cartilage reconstruction[34] but we define that passage 2 (and always lower than 5) is a reasonable limit to preserve the biological properties of chondrocytes at maximum before re-implantation. We also describe that MCs possess an inferior growth curve than rib or healthy chondrocytes in line with data from other authors[14] but, surprisingly, we found that this effect is merely a delay because they can reach the same values of growth than rib or healthy chondrocytes after 5 days of culture. Our experiments using MCs demonstrated that the optimal chondrocyte growth medium was Ham's medium supplemented with 10% FBS and b-FGF. Indeed, b-FGF is essential not only for enhanced chondrocyte proliferation,[35] as we have also observed, but also for controlling and maintaining the cartilage homeostasis.[36] Literature describes that it is required to obtain 150 million cells at least for seeding an entire engineered 3D-printed or molded

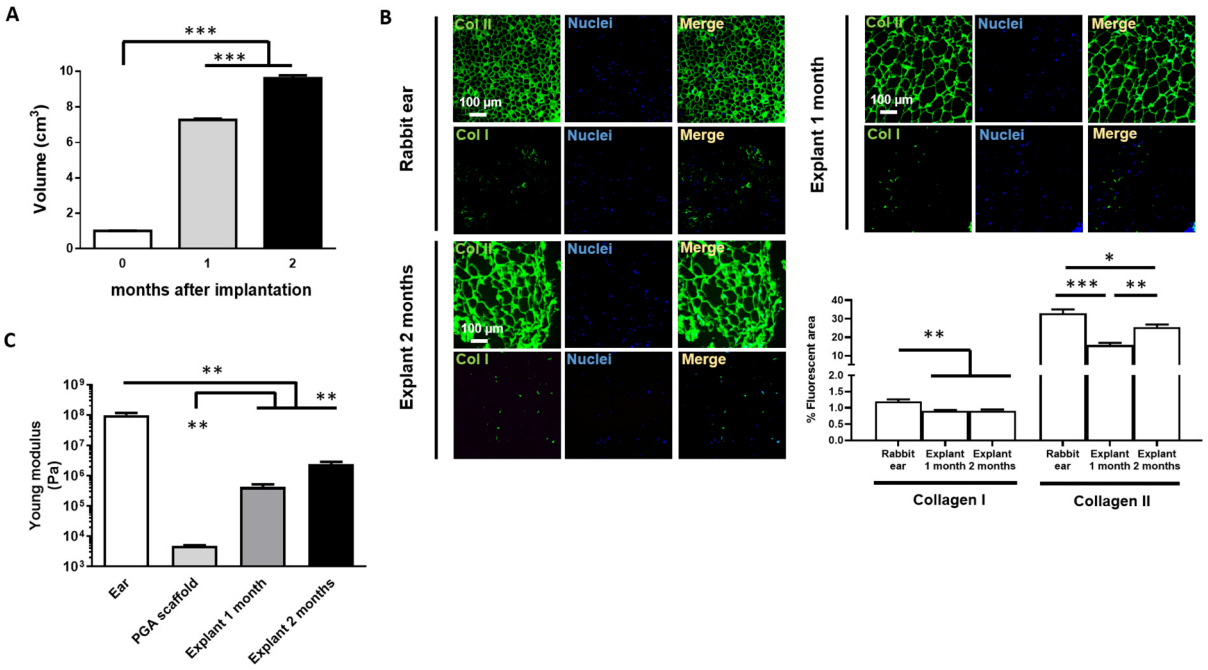

Fig. 8 Properties of explants obtained from implanting subcutaneously PGA scaffolds seeded with rabbit chondrocytes in immunocompetent rabbits. (A) Volume of cartilage explants obtained 1 or 2 months after subcutaneous implantation of PGA scaffolds seeded with rabbit chondrocytes in immunocompetent rabbits. (B) Immunofluorescent staining and fluorescent area percentage quantification of collagen I and II in rabbit ear cartilage and explants obtained 1 and 2 months after subcutaneous implantation of PGA scaffolds seeded with rabbit chondrocytes in immunocompetent rabbits (C) Young Modulus quantification in rabbit cartilage explants to analyse mechanical strength and elasticity compared to a rabbit ear or acellular PGA scaffold. ***$p < 0.001$; **$p < 0.01$. Analyse mechanical strength and elasticity compared to a rabbit ear or acellular PGA scaffold. ***$p < 0.001$; **$p < 0.01$. Analyse mechanical strength and elasticity compared to a rabbit ear or acellular PGA scaffold. ***$p < 0.001$; **$p < 0.01$.

ear.[37,38] Massive expansion is essential for that number of cells. However, it is impossible to reach such cell numbers with only two passages (needed for keeping the chondrocyte phenotype). Therefore, we seeded 50 million chondrocytes per PGA scaffold and aimed at using the own host subcutaneous tissue as a bioreactor to build a bigger cartilaginous tissue using chondrocytes from rabbit origin (and from human in the future), which grow adequately in PGA scaffolds maintaining the morphological and biological properties.

Investigations have increasingly focused on MCs isolation, expansion, and integration with precision in scaffolds using MCs alone or in combination with MSCs and have made their way from animal models into clinical trials.[25,27,28,39] We investigated the appropriateness of culturing chondrocytes with MSCs as these latter can secrete trophic factors[40] that enhance the chondrogenic phenotype and cartilage formation *in vitro* and *in vivo*.[25] Our results corroborated that the addition of MSCs to a chondrocyte cell culture in a 50 : 50 ratio optimizes the synthesis of chondrogenic proteins such as elastin, proteoglycans and cell growth. However, when this combination of rabbit chondrocytes and MSCs in PGA scaffolds was used for subcutaneous implantation in immunosupressed mice, these implants failed to grow significantly after 2 months of implantation, and the addition of MSCs had no real impact. In contrast, other authors have successfully achieved certain cartilage growth using 100% porcine chondrocytes in nude mice.[41] In any case, this mouse model has shown clear limitations to assess whether implants of PGA scaffolds seeded with chondrocytes may be used to obtain a high amount of cartilaginous tissue to reconstruct a full-size human ear from a small initial implant. This can be explained in part by two main reasons: mice are small animals with a low dorsal surface area for cartilaginous tissue growth and expansion; and the absence of the immune system in nude mice may affect cartilage growth since immune cells are essential for any tissue regeneration.[42–45] The use of immunocompetent rabbits helped to solve both issues. Our main objective was to employ the subcutaneous tissue as a bioreactor to generate enough cartilage mass from a small sample to mold a full-shape ear. Although rabbit chondrocytes seeded on PGA scaffolds have traditionally showed the production of a cartilaginous tissue in a closed bioreactor system,[46] our hypothesis was that the subcutaneous tissue of a patient could be a biological bioreactor to accommodate chondrocyte-seeded PGA scaffolds and to produce cartilage. We demonstrated that we could obtain enough cartilaginous mass in 4 weeks to mold a full-shape ear *via* subcutaneous growth of chondrocyte-seeded PGA scaffolds compared to another report requiring up to 20 weeks.[15] This cartilaginous tissue demonstrated biofunctional and mechanical properties similar to an ear cartilage. Indeed collagen II matrix resulted surprisingly complex and with a polygonal shape very similar to the ear cartilage. This specific patterning could be caused by the mechan-

ical stress in the dorsal subcutaneous tissue due to the animal movements. Our experiments using chondrocyte-seeded scaffolds under continuous shear stress also revealed an increased synthesis of collagen I with a preservation of high collagen II synthesis. There are investigations pointing to mechanical forces as inducers of epithelial–mesenchymal transition,[47–49] and therefore to the collagen I synthesis. In this scenario, mechanical stress in the subcutaneous tissue might be enough to force some chondrocytes to express collagen I and surround the cartilaginous tissue by fibrous materials to give mechanical strength and support for the newly formed tissue. Indeed, we found some areas with collagen I in both 1- and 2-month explants as well as in the rabbit ear cartilage. Therefore, although a low content of collagen I seems necessary to compose the ear cartilage, following this rationale, MSCs are not necessary for a complete cartilage regeneration in immunocompetent large size animals and consequently in humans. Our surgical experience working with costal cartilage fragments for ear reconstruction suggests that subcutaneous implantation leaves cartilage biologically preserved and covered with a thin layer of connective tissue over time, in line with the findings of the present study. The most convenient location to implant the chondrocyte-seeded PGA scaffold in humans is the groin area, which is easy to access through an incision in the groin crease. Our idea is that a small subcutaneous and supra-aponeurotic pocket could be created there where the cell-seeded PGA scaffold could be placed. The site would be protected and aesthetic allowing a normal life. After about 2–6 months, the cartilaginous backbone could be removed from the inguinal subcutaneous site, molded to shape an ear, and placed subcutaneously in the final auricular site.

The novelty of our study lies in the fine-tuning of the critical conditions for the growth of a cartilaginous tissue from subcutaneous implantation of PGA scaffolds seeded with autologous chondrocytes, which are isolated from a small biopsy of ear cartilage. First, we establish the limits of passage 2 and the requirement of b-FGF to preserve the phenotype of chondrocytes isolated from either patients with microtia or rabbits. Second, we describe that folding twice a chondrocyte-seeded PGA layer is beneficial for fast and successful cartilage growth in the subcutaneous tissue since allows a multi-layer 3D cell environment. These findings and premises will lay the ground for the design of new generation auricular surrogates. This investigation may also help to the optimization of implant protocols that are currently using state-of-the-art 3D printing technologies for auricular reconstruction.[50]

Conclusions

In summary, isolated chondrocytes begin to lose a cartilage biological phenotype rapidly after two passages during *in vitro* expansion but can grow rapidly at 10% FBS with b-FGF in PGA scaffolds retaining strong cartilage formation ability. The protocol of isolation and re-implantation using folded chondrocyte-seeded PGA scaffolds described here successfully promoted cartilage growth in the subcutaneous environment of immunocompetent rabbits to obtain enough cartilaginous material to mold and mimic a biofunctional full-size ear-shaped cartilage. This regenerative technology is also applicable to the reconstruction of auricle fragments of varying size with lower cost and needs thus avoiding the use of 3D-printers or the isolation of MSCs. In future studies, we will translate our findings to clinical use. The technology developed in the current study may also help to promote the clinical translation of other cartilage regeneration (nasal back and wing, palate fistula, nasal vestibule fistula, eyelids, or other reconstructive applications) where the size of the required cartilage implant is smaller and the shape simpler.

Author contributions

P. M.-L., O. B., R. Z., G. M., S. C., A. L.-S., F. G.-P., and M. L.-M. performed the experiments and analyzed the data. F. J. P. F. obtained human samples and Ethical approval from Hospital Sant Joan de Deu and participated in surgical procedures. P. M.-L., C. R., A. G., J. M., E. R. E. and M. B. designed the experiments and wrote the manuscript.

Abbreviations and acronyms

b-FGF	Basic fibroblast growth factor
ECM	Extracellular matrix
FBS	Fetal bovine serum
MCs	Human microtia chondrocytes
MSC	MSC
PGA	Polyglycolic acid

Ethical statement

All animal procedures were performed in accordance with the Guidelines for Care and Use of Laboratory Animals of the United States' Animal Welfare Act and Animal Welfare Regulations code and approved by the Animal Ethics Committee of the Massachusetts Institute of Technology. Human samples were obtained after approval by the Clinical Ethics Committee at the Hospital Sant Joan de Déu in Barcelona and Boston Children's Hospital.

Conflicts of interest

The authors declare no competing financial interests.

Acknowledgements

We acknowledge support provided by the David H. Koch Institute for Integrative Cancer Research at the Massachusetts

Institute of Technology for providing access to multiphoton microscopy used for this study. M. B. was supported in part by Fundació Empreses IQS, by La Caixa Foundation, by the Asociación Española de Microtia and the MIT-Spain program, and by two grants from the Spanish Ministry of Economy, SAF2013-43302-R and SAF2017-84773-C2-1-R. E. R. E. and this work was supported in part by a grant (R01 HL 161069) from the National Institutes of Health. P. M.-L. was supported by the Ministerio de Ciencia, Innovación y Universidades (grant PID2021-123426OB-I00) co-funded by the European Regional Development Fund (ERDF)-"A way to make Europe", and the Ramón y Cajal Program 2018 (Ministerio de Ciencia, Innovación y Universidades, Reference: RYC2018-023971-I). The Centro de Investigación Biomédica en Red de Enfermedades Hepáticas y Digestivas (CIBERehd) is funded by the Instituto de Salud Carlos III. A. G. acknowledges the support from Regenear and the Asociación Española de Microtia.

References

1 D. V. Luquetti, C. L. Heike, A. V. Hing, M. L. Cunningham and T. C. Cox, *Am. J. Med. Genet., Part A*, 2012, **158A**, 124–139.
2 D. V. Luquetti, E. Leoncini and P. Mastroiacovo, *Birth Defects Res., Part A*, 2011, **91**, 813–822.
3 M. Shirazi, E. Abbariki, R. Pirjani, S. Akhavan and E. Dastgerdy, *J. Obstet. Gynaecol. Res.*, 2015, **41**, 975–978.
4 S. Tripathee, M. Xiong and J. Zhang, *World J. Plast. Surg.*, 2019, **8**, 324–330.
5 J. J. Cubitt, L. Y. Chang, D. Liang, J. Vandervord and D. D. Marucci, *J. Paediatr. Child Health*, 2019, **55**, 512–517.
6 R. Karuppal, *J. Orthop.*, 2017, **14**, A1–A3.
7 J. Melrose, C. Shu, J. M. Whitelock and M. S. Lord, *Matrix Biol.*, 2016, **52–54**, 363–383.
8 G. A. Di Lullo, S. M. Sweeney, J. Korkko, L. Ala-Kokko and J. D. San Antonio, *J. Biol. Chem.*, 2002, **277**, 4223–4231.
9 K. Gelse, E. Poschl and T. Aigner, *Adv. Drug Delivery Rev.*, 2003, **55**, 1531–1546.
10 R. Mayne, *Arthritis Rheum.*, 1989, **32**, 241–246.
11 C. M. Kielty, M. J. Sherratt and C. A. Shuttleworth, *J. Cell Sci.*, 2002, **115**, 2817–2828.
12 C. Nabzdyk, L. Pradhan, J. Molina, E. Perin, D. Paniagua and D. Rosenstrauch, *In Vivo*, 2009, **23**, 369–380.
13 B. Gurer, S. Cabuk, O. Karakus, N. Yilmaz and C. Yilmaz, *J. Orthop. Surg. Res.*, 2018, **13**, 107.
14 Y. Gu, N. Kang, P. Dong, X. Liu, Q. Wang, X. Fu, L. Yan, H. Jiang, Y. Cao and R. Xiao, *J. Tissue Eng. Regener. Med.*, 2018, **12**, e1737–e1746.
15 Y. Itani, S. Asamura, M. Matsui, Y. Tabata and N. Isogai, *Plast. Reconstr. Surg.*, 2014, **133**, 805e–813e.
16 R. Balamurugan, M. Mohamed, V. Pandey, H. K. Katikaneni and K. R. Kumar, *J. Contemp. Dent. Pract.*, 2012, **13**, 521–527.
17 J. Y. Jang, Y. C. Shin, Y. Han, J. S. Park, H. S. Han, H. K. Hwang, D. S. Yoon, J. K. Kim, Y. S. Yoon, D. W. Hwang, C. M. Kang, W. J. Lee, J. S. Heo, M. J. Kang, Y. R. Chang, J. Chang, W. Jung and S. W. Kim, *JAMA Surg.*, 2017, **152**, 150–155.
18 H. Kasahara and I. Hayashi, *J. Cardiothorac. Surg.*, 2014, **9**, 121.
19 K. Torikai, H. Ichikawa, K. Hirakawa, G. Matsumiya, T. Kuratani, S. Iwai, A. Saito, N. Kawaguchi, N. Matsuura and Y. Sawa, *J. Thorac. Cardiovasc. Surg.*, 2008, **136**, 37–45.
20 L. Bruder, H. Spriestersbach, K. Brakmann, V. Stegner, M. Sigler, F. Berger and B. Schmitt, *J. Funct. Biomater.*, 2018, **9**(4), 64.
21 L. Cui, Y. Wu, L. Cen, H. Zhou, S. Yin, G. Liu, W. Liu and Y. Cao, *Biomaterials*, 2009, **30**, 2683–2693.
22 N. D. Miller and D. F. Williams, *Biomaterials*, 1984, **5**, 365–368.
23 P. Harrison, T. Hopkins, C. Hulme, H. McCarthy and K. Wright, *Methods Mol. Biol.*, 2023, **2598**, 9–19.
24 H. Methe, M. Balcells, C. Alegret Mdel, M. Santacana, B. Molins, A. Hamik, M. K. Jain and E. R. Edelman, *Am. J. Physiol.: Heart Circ. Physiol.*, 2007, **292**, H2167–H2175.
25 Y. Yang, H. Lin, H. Shen, B. Wang, G. Lei and R. S. Tuan, *Acta Biomater.*, 2018, **69**, 71–82.
26 C. Hegert, J. Kramer, G. Hargus, J. Muller, K. Guan, A. M. Wobus, P. K. Muller and J. Rohwedel, *J. Cell Sci.*, 2002, **115**, 4617–4628.
27 B. P. Cohen, J. L. Bernstein, K. A. Morrison, J. A. Spector and L. J. Bonassar, *PLoS One*, 2018, **13**, e0202356.
28 L. Zhang, A. He, Z. Yin, Z. Yu, X. Luo, W. Liu, W. Zhang, Y. Cao, Y. Liu and G. Zhou, *Biomaterials*, 2014, **35**, 4878–4887.
29 C. B. Knudson and W. Knudson, *Semin. Cell Dev. Biol.*, 2001, **12**, 69–78.
30 H. Li, S. Shen, H. Fu, Z. Wang, X. Li, X. Sui, M. Yuan, S. Liu, G. Wang and Q. Guo, *Stem Cells Int.*, 2019, **2019**, 9671206.
31 A. Longoni, L. Knezevic, K. Schepers, H. Weinans, A. Rosenberg and D. Gawlitta, *npj Regener. Med.*, 2018, **3**, 22.
32 P. Melgar-Lesmes, M. Balcells and E. R. Edelman, *Gut*, 2017, **66**, 1297–1305.
33 S. S. Kang, Y. Guo, D. Y. Zhang and D. Y. Jiang, *China Med. J.*, 2015, **128**, 2208–2214.
34 J. L. Bernstein, B. P. Cohen, A. Lin, A. Harper, L. J. Bonassar and J. A. Spector, *Ann. Plast. Surg.*, 2018, **80**, S168–S173.
35 Y. Li, Q. Fan, Y. Jiang, F. Gong and H. Xia, *Exp. Ther. Med.*, 2017, **14**, 2657–2663.
36 M. B. Ellman, D. Yan, K. Ahmadinia, D. Chen, H. S. An and H. J. Im, *J. Cell. Biochem.*, 2013, **114**, 735–742.
37 D. A. Bichara, N. A. O'Sullivan, I. Pomerantseva, X. Zhao, C. A. Sundback, J. P. Vacanti and M. A. Randolph, *Tissue Eng., Part B*, 2012, **18**, 51–61.
38 S. Landau, A. A. Szklanny, M. Machour, B. Kaplan, Y. Shandalov, I. Redenski, M. Beckerman, O. Harari-Steinberg, J. Zavin, O. Karni-Katovitch, I. Goldfracht,

I. Michael, S. D. Waldman, S. I. Duvdevani and S. Levenberg, *Biofabrication*, 2021, **14**(1), 015010.
39 G. Zhou, H. Jiang, Z. Yin, Y. Liu, Q. Zhang, C. Zhang, B. Pan, J. Zhou, X. Zhou, H. Sun, D. Li, A. He, Z. Zhang, W. Zhang, W. Liu and Y. Cao, *EBioMedicine*, 2018, **28**, 287–302.
40 Z. Wang, H. Le, Y. Wang, H. Liu, Z. Li, X. Yang, C. Wang, J. Ding and X. Chen, *Bioact. Mater.*, 2022, **11**, 317–338.
41 A. Lohan, U. Marzahn, K. El Sayed, A. Haisch, B. Kohl, R. D. Muller, W. Ertel, G. Schulze-Tanzil and T. John, *Histochem. Cell Biol.*, 2011, **136**, 57–69.
42 P. Abnave and E. Ghigo, *Semin. Cell Dev. Biol.*, 2019, **87**, 160–168.
43 A. V. Pechersky, V. I. Pechersky, M. V. Aseev, A. V. Droblenkov and V. F. Semiglazov, *J. Stem Cells*, 2016, **11**, 69–87.
44 P. Melgar-Lesmes and E. R. Edelman, *J. Hepatol.*, 2015, **63**, 917–925.
45 L. Jia, P. Zhang, Z. Ci, W. Zhang, Y. Liu, H. Jiang and G. Zhou, *Front. Bioeng. Biotechnol.*, 2021, **9**, 667161.
46 N. S. Dunkelman, M. P. Zimber, R. G. Lebaron, R. Pavelec, M. Kwan and A. F. Purchio, *Biotechnol. Bioeng.*, 1995, **46**, 299–305.
47 R. L. Heise, V. Stober, C. Cheluvaraju, J. W. Hollingsworth and S. Garantziotis, *J. Biol. Chem.*, 2011, **286**, 17435–17444.
48 H. P. Lee, L. Gu, D. J. Mooney, M. E. Levenston and O. Chaudhuri, *Nat. Mater.*, 2017, **16**, 1243–1251.
49 L. E. Scott, S. H. Weinberg and C. A. Lemmon, *Front. Cell Dev. Biol.*, 2019, **7**, 135.
50 N. Bhamare, K. Tardalkar, P. Parulekar, A. Khadilkar and M. Joshi, *Biomed. Mater.*, 2021, **16**(5), 055008.